Desalination and Water Treatment
www.deswater.com

doi: 10.5004/dwt.2017.21473

96 (2017) 104–111
November

Study on the adsorption performance for fluoride by mesoporous silica loaded rare earth lanthanum (Ms-La) material

Rui Wang[a,†], Guizhen Li[a,†], Yongjun Yang[a], Li Shu[b], Veeriah Jegatheesan[b], Hongbin Wang[a,*], Min Yang[a,*]

[a]*School of Chemistry and Environment, Yunnan Minzu University, Kunming, Yunnan 650500, China, emails: 392639402@qq.com (R. Wang), 3258657752@qq.com (G.Z. Li), 1060656032@qq.com (Y.J. Yang), 595530820@qq.com (H.B. Wang), 826677468@qq.com (M. Yang)*
[b]*School of Civil, Environmental and Chemical Engineering, RMIT University, Melbourne, VIC 3000, Australia, emails: li.shu846@gmail.com (L. Shu), jega.jegatheesan@rmit.edu.au (V. Jegatheesan)*

Received 1 March 2017; Accepted 21 September 2017

ABSTRACT

In this paper, the Ms-La materials for the fluoride removal performance were characterized using scanning electron microscopy (SEM), X-ray diffractometer (XRD), Fourier-transform infrared spectrometer (FTIR) and the thermogravimetric analysis-differential temperature analysis (TG-DTA). And the effect of the different dosage, adsorption time, adsorption temperature, pH and coexistence of anions in water was also investigated. The adsorption performance and capacities of Ms-La were investigated through adsorption kinetics and adsorption isotherm tests. The results showed that the maximum fluorine removal efficiency on the loaded materials were that the adsorbent dosage, pH value and the adsorption time were 1.2 g/L, 3.0 and 180 min, respectively. Dynamics research results showed that the fluoride removal process by Ms-La was in accordance with pseudo-second-order kinetic model and the effect of temperature on adsorption was very little. Isothermal adsorption results showed that the fluorine ion adsorption process of Ms-La was in accordance with the Langmuir isotherm adsorption model, and the maximum adsorption capacity was 19.85 mg/g. The adsorption process of Ms-La is mainly irreversible chemical adsorption, and the main reaction is that the active component of lanthanum carbonate has ion exchange with fluoride ion to generate $LaCO_3F$.

Keywords: Fluoride removal; Modification; Adsorption

1. Introduction

Fluorine is one of the necessary trace elements for human and other creatures. However, excessive intake will have negative effects, which may cause fluorosis, dental fluorosis, or even death [1]. The dental fluorosis is very common in many impoverished mountainous areas, because there is serious fluorine pollution in the groundwater, the fluorine content of which highly exceeds the standard. Due to the relatively backward local economic conditions, the pollution brings serious damage to residents and crops [2]. In recent years, with the growth of people's environmental protection consciousness and food safety consciousness, people are paying more and more attention to deal with fluorine pollution, the safety of food and the drinking water. Such studies are looking for a fluoride removal material

* Corresponding author.

† Authors contributed equally to this work.

Presented at the 9th International Conference on Challenges in Environmental Science & Engineering (CESE-2016), 6–10 November 2016, Kaohsiung, Taiwan, 2016

with high efficiency, energy savings, and environmental protection, etc. It has become research hotspot now both home and abroad [3]. At present, there are many methods to remove the fluoride in industrial wastewater, such as absorption, sedimentation, ion exchange, membrane separation, electroosmosis, electric agglomerate, and filtration. The adsorption method is the most effective of all for fluoride removal because of its advantages such as a little secondary pollution, high efficiency, simple, and safe [4].

Mesoporous materials (Ms) has a special structure, which has excellent characteristics such as highly ordered channel, particle size rules, large specific surface area, and the size of diameter within (2–100 nm), etc. It has the widespread application prospect in the fields of catalysis, adsorption, separation, purification, nanometer materials, and environmental [5–7]. Depending on the different pore structure, it can be divided into ordered and disordered structure materials, and according to its chemical composition, it can be divided into the silicon-based and the non-silicon-based Ms [8]. The skeleton of the non-silicon-based Ms is mainly made of carbon, Al_2O_3, transition metal oxides, phosphate and sulfides. Moreover, silicon-based Ms can be divided into pure silicon and doped silicon, which is mainly made up of silicon and oxygen [9]. Ms provides the convenient condition for its modification because of its characteristics such as high porosity, hole adjustable, and large specific surface. According to the modified properties, Ms can be divided into organic functional modification, heteroatomic substitution and loading of active component [10]. Rare earth element is one of the most important loading of active component. Lanthanide is rather special in the location of the Periodic Table and has big atomic radius, so it is easy to lose electrons and strong metal activity. Hence, lanthanide has strong affinity ability and is easy to form a high coordination number of ligand with oxygen, fluorine, etc [11]. The purpose of this paper is to find a good performance, environmental protection, and high-efficient fluorine removal agent. Rare earth metal lanthanum, an active component, is assembled into the Ms materials by loaded methods. This will improve its utilization rate and performance in the fields of adsorption and catalysis because the loaded method will make the active components better dispersed and smaller particle size. At the same time, due to the pore-limiting effect of Ms and the size effect of nanoparticles, Ms-La has high activity and selectivity [12]. In this paper, the influential factors of preparation conditions of Ms-La such as the amount of adsorbent, adsorption time, initial solution pH, temperature on the fluoride removal were studied.

2. Experimental

2.1. Materials and reagents

Hexahydrate lanthanum nitrate ($La(NO_3)_3{\cdot}6H_2O$, 98%) purchased from Tianjin Institute of Fine Chemical Industry, China; Sodium fluoride (NaF, 98%) purchased from Chengdu Chemical Reagent Factory, China; sodium bicarbonate ($NaHCO_3$) and sodium nitrate ($NaNO_3$) purchased from Tianjin Damao Chemical Reagent Factory, China; All the reagents were at analytical grade.

2.2. Preparation of Ms-La

Based on the study by Li et al. [13], lanthanum an active component was loaded into the Ms materials. With 0.08 mole ratio of La/Si, lanthanum was dissolved in silica dispersion solution, and then the precipitant Na_2CO_3 was slowly added to the above mixed solutions under the stirring condition. After continuously stirring for 10 h, it was filtered, washed and dried, the Ms-La had been successfully prepared.

2.3. Evaluation method

2.3.1. Analysis method

The determination method for fluorine ion content is in accordance with the "water and water quality monitoring analysis method" (GB7484-1987) of the ion selective electrode method [14].

2.3.2. Adsorption experiment

Adsorption experiments were carried out by batch adsorption method in a condition of 25°C in a shaker at 200 rpm for 3 h. Then, 0.1000 g of Ms-La was added into conical flask and 50 mL of 10 mg/L fluoride ion solution (F^-) was transferred in this bottle. After centrifugal separation, the residual concentration of fluoride ion in the supernatant fluid was determined. The removal rate R (%) and adsorption capacity Q (mg/g) were used to evaluate the performance of rare earth modified Ms materials. The removal rate of R (%) is as follows:

$$R\ (\%) = \frac{C_0 - C_t}{C_0} \times 100\% \tag{1}$$

Adsorption capacity of Q (mg/g)

$$Q(\mathrm{mg \cdot g^{-1}}) = \frac{(C_0 - C_t) \times V}{m \times 1000} \tag{2}$$

The initial concentration of fluoride ion (mg/L) in the wastewater is C_0; the residual concentration of fluoride ion (mg/L) in wastewater is C_t; the adsorbent for fluoride ion adsorption capacity (mg/g) is Q; the amount of fluoride ion solution (mL) is V; the adsorbent amount (g) is M.

2.4. Study on the adsorption performance for fluoride by Ms-La

2.4.1. Effect of adsorbent dosage on fluoride adsorption

Adsorption experiments were carried out in a shaking table in a condition of 25°C and the speed of 200 rpm for 3 h. Different dosage (0.1–4.0 g/L) of Ms-La was added into adsorption bottle, and 5 mL of fluoride ion solution (F^-) was added to this bottle whose concentration was 10 mg/L. After centrifugal separation, the residual concentration of fluoride ion in the supernatant fluid was determined.

2.4.2. Effect of initial solution pH on the fluoride adsorption

The above optimal adsorbent dosage was added into adsorption bottle, and 50 mL of 10 mg/L of fluoride ion solution (F^-) in this bottle whose range of pH was 2–12. After centrifugal separation, the residual concentration of fluoride ion in the supernatant fluid was determined.

2.4.3. Effect of adsorption time on the fluoride adsorption

The above optimal adsorbent dosage was added into adsorption bottle, and transferred 50 mL of fluoride ion solution (F^-) in this bottle whose concentration was 10 mg/L. Adsorption experiments were carried out at different times from 10 to 300 min, as well, by following the same steps mentioned above.

2.4.4. Effect of temperature on the fluoride adsorption

Adsorption experiments were carried out at different temperature conditions (25°C, 35°C, 45°C), the speed of 200 rpm and the time (10–300 min), as well, by following the same steps mentioned earlier.

2.4.5. The interference experiment of the coexistence anion on the effect for adsorption of fluoride

A series of mixture simulated solution of coexistent anion solutions (HCO_3^-, Cl^-, NO^{3-}, SO_4^{2-}, PO_4^{3-}) with initial fluoride concentration of 10 mg/L were prepared. Under the optimal conditions of adsorption experiments, 0.060 g of adsorbent was added into 50 mL of the mixture simulated solution. By following the same steps mentioned earlier.

2.4.6. The isothermal experiment

Adsorption experiments using a shaking table at different temperature conditions (25°C, 35°C, 45°C) and the speed of 200 rpm for 3 h. The above optimal amount of adsorbent was added into adsorption bottle, and transferred 50 mL of fluoride ion solution (F^-) in this bottle whose concentration was 2–80 mg/L, as well, by following the same steps mentioned earlier. The adsorption isotherms were plotted and drawn by using Langmuir adsorption model and Freundlich adsorption model.

2.5. Characterization of the changes of the Ms-La before and after adsorption

Scanning electron microscopy (SEM), X-ray diffractometer (XRD), Fourier-transform infrared spectrometer (FTIR), TG-DTA were used to investigate the changes of the Ms-La before and after adsorption, and the adsorption mechanism was explained. Morphology of prepared materials was observed by SEM (FEI-Nova, NanoSEM450, USA). The structures of the materials were characterized by XRD (Rigaku, Japan) with Cu Ka radiation (45 kV, 250 mA) and a continuous scan mode was employed with a scan rate of 10 min^{-1}. FTIR images were obtained by a spectrometer (NICOLETIS10) with the powder samples embedded in KBr disks. The prepared materials were analyzed by the thermogravimetric analysis-differential temperature analysis (TG-DTA, STAA49F31, differentia Germany).

3. Results and discussion

3.1. The adsorption experiment on the F^- removal by Ms-La

3.1.1. Effect of adsorbent dosage

The effect of the dosage of Ms-La on the F^- removal is shown in Fig. 1. From Fig. 1, it can be seen that the removal rate of F^- increased gradually with the increase of the dosage of adsorbed material. The removal rate of F^- increased linearly with the increase of the dosage of composite materials which was in the range of 0.1–0.8 g/L. The removal rate (%) was 83% when the dosage of adsorbent was 1.2 g/L. Then it continued to increase the dosage of adsorbent, F^- removal rate increased less and gradually tended to be gentle. After the dosage of adsorbent increased to 1.4 g/L, the remaining F^- concentration in water was lower than the upper limit value of 1.5 mg/L of the WHO on F^- in drinking water limit and closed to the limit value of 1.0 mg/L of the Chinese in drinking water [15]. Therefore, l.2 g/L adsorbent dosage was selected as optimal dosage.

3.1.2. Effect of initial solution pH

The effect of initial solution pH on the F^- removal is shown in Fig. 2. The results showed that there was a wide

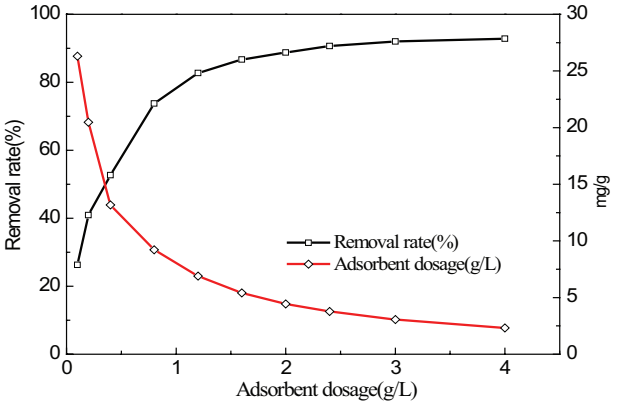

Fig. 1. Effect of adsorbent dosage on defluorination efficiency.

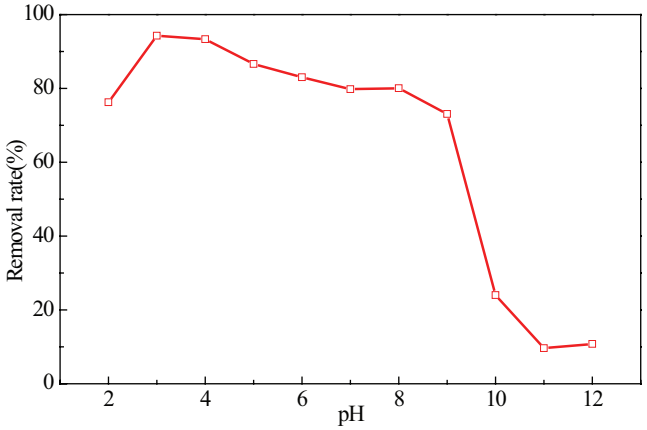

Fig. 2. Effect of initial solution pH on the removal of fluoride.

range of pH from 2.0 to 8.0 in the F^- adsorption. The adsorbent had better adsorption effect on F^- in the acidic solution. The removal efficiency of F^- increased with the increase of initial pH value of solution in the pH range 2.0–3.0. The best removal effect was 94.29% and the concentration of F^- was 0.57 mg/L in the pH value of 3.0. The removal rate decreased more slowly in the pH range 3.0–9.0. When the pH value of solution increased 9.0, the removal rate was kept at about 75%. After the pH value was higher than 9.0, the removal rate decreased sharply, and until it was only 10%. These phenomena can be explained as follows: First, when the pH value was less than 3.0, the hydrofluoric acid of solution leads to the fact that the effective component $La_2(CO_3)_3$ of adsorbent was destroyed to generate LaF_3. On the other hand, the materials of the isoelectric point were 3.0. When the pH value was higher than 3.0 in the initial solution, the increase of pH caused that the adsorbent surface potential decreased and adsorption agent surface had negatively charge, so it had the repelling effect on F^- and the effect of removal fluoride was decreased; Second, OH^- and F^- in the solution formed competitive adsorption under alkaline condition, thus the number of active sites which were used to adsorb F^- was decreased. Therefore, the pH value of 3.0 was selected as the optimal pH [16].

3.1.3. Effect of adsorption time and the initial F^- concentration

The effects of adsorption time and the initial F^- concentration of 10, 30 and 50 mg/L on adsorption performance of Ms-La are shown in Fig. 3. From Fig. 3, we can see that the adsorption process accelerated quickly in the first half, and adsorption tended to be slow down in the second half. The reason is that there were the higher concentration of F^- and the more effective sites of adsorbent at the beginning of adsorption. As the adsorption process went on, F^- concentration gradually decreased, and the site was gradually occupied. At different initial concentrations, the adsorption capacity of fluoride adsorbing on the adsorption material increased quickly at first, and then tended to be stable at the initial stage of adsorption. The adsorption equilibrium time was relatively backward, with the increase of the initial concentration. When the adsorption was up to 120 min, the adsorption gradually tended to be balanced. Hence, the adsorption time was 180 min.

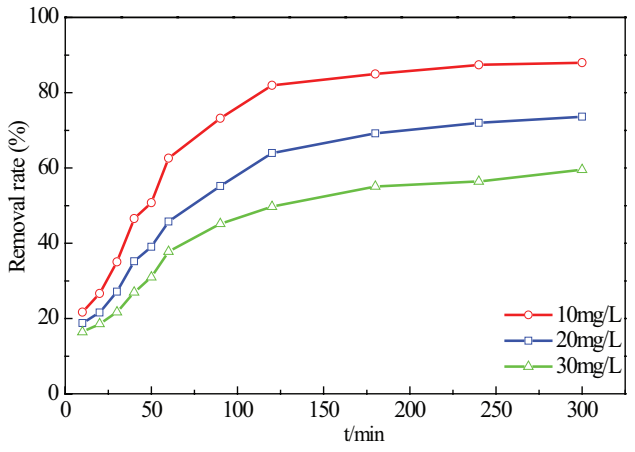

Fig. 3. Effect of different concentrations of time.

3.1.4. Effect of temperature

The effects of three different temperatures (25°C, 35°C, 45°C) on F^- removal are shown in Fig. 4. According to Fig. 4, the changes of the removal rate were faster with the increase of temperature and the increase in temperature would benefit the adsorption before the adsorption equilibrium. It illustrated that the adsorption reached equilibrium after 150 min, and the temperature had less effect on the adsorption, which indicated that the thermal effect of the adsorbent on the F^- adsorption process was very little.

3.1.5. Effect of the interference experiment of the coexistence anion

There are other anions in water, which can compete with the F^- in the process of adsorption. The effects of these five kinds of anions (HCO_3^-, Cl^-, NO^{3-}, SO_4^{2-}, PO_4^{3-}) whose concentration was ranged from 10 to 400 mg/L on the F^- removal in this interference experiment are shown in Fig. 5. The results show that the two anions (PO_4^{3-} and HCO_3^-) had a significant interference on the adsorption after the PO_4^{3-} and HCO_3^- concentration rose to a certain degree, the effect was greatly reduced with the increase of the two anions concentration, and other three kinds of anions had no effect on this adsorption. The interference effect of PO_4^{3-} was greater than that of HCO_3^-. The removal rate only reached 23% when the concentration of PO_4^{3-} was up to 60 mg/L. The main reason is that the coexistent anion will form competitive adsorption with F^- and occupied a part of the active sites of Ms-La,

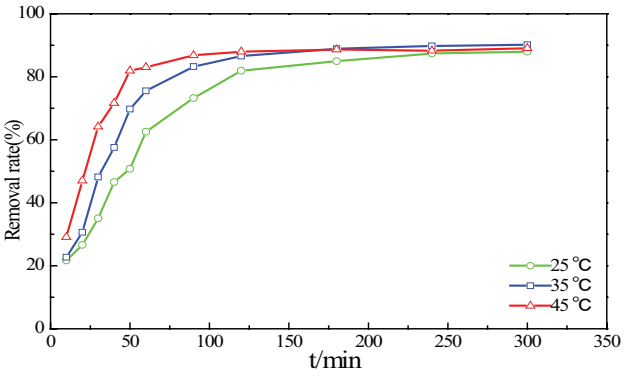

Fig. 4. Effect of temperature.

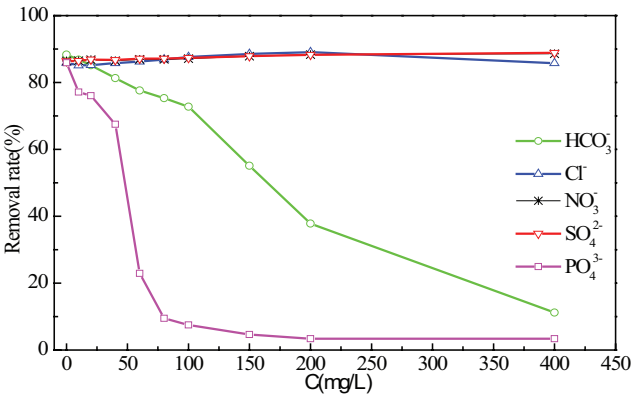

Fig. 5. Effect of common anion.

so that common anion could make the effect of F^- removal worse when the PO_4^{3-} and HCO^{3-} concentration rose to be 50 and 100 mg/L, respectively. Lanthanide ions and phosphate ions generated chelating effect, and phosphate ions can replace carbonate ions. Therefore, the number of active sites was reduced and it had no advantage for the F^- removal [17].

3.2. Characterization of the changes of the Ms-La before and after adsorption

3.2.1. SEM analysis

In order to observe the changes of the morphology of the molar ratio of La/Si before and after adsorption, the SEM results are shown in Fig. 6. Figs. 6(a)–(c) represent Ms-La at La/Si ratio of 0.08 before adsorption, pure-$La_2(CO_{3)3}$ and Ms-La at La/Si ratio of 0.08 after adsorption, respectively. The morphology of pure-$La_2(CO_{3)3}$ is sheet accumulation from Fig. 6(b). It can be seen that it has a small amount of lanthanum carbonate on the surface of Ms-La at the La/Si = 0.08 before adsorption from Fig. 6(a). Compared with Fig. 6(a), the shape of Ms-La after adsorption changed obviously, the original small amount of sheet deposits basically disappeared, and small white particles were formed from Fig. 6(c). This indicated that adsorption agents and adsorbate may react in the adsorption process [18].

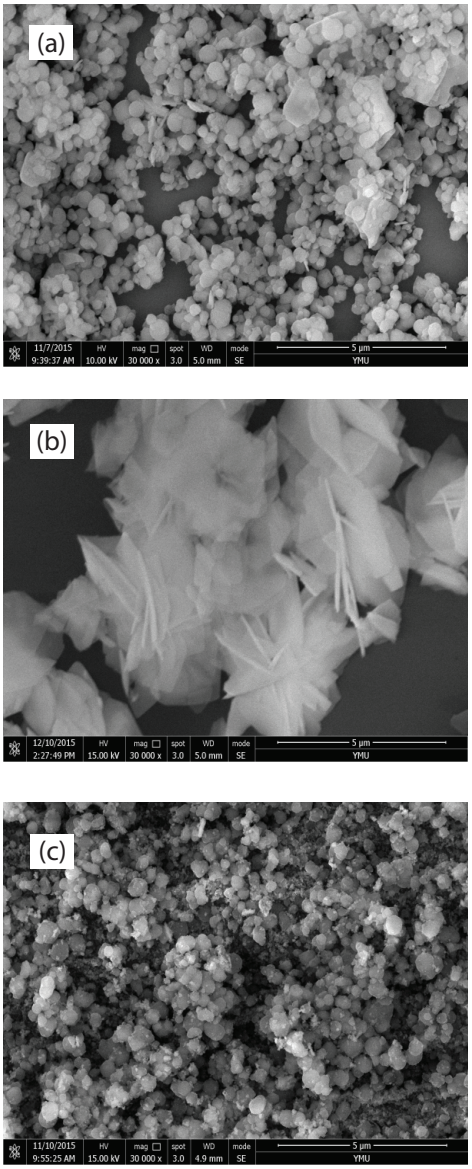

Fig. 6. SEM before and after adsorption of the molar ratio of La/Si.

3.2.2. XRD analysis

In order to investigate the crystal phase structure, the XRD spectra of Ms (SiO_2 carrier), pure-$La_2(CO_3)_3$ and Ms-La are recorded in Fig. 7. The Ms-La still remained the original characteristics of diffraction peak, and the peak position had no bias shift. Because the content of $La_2(CO_3)_3$ was lower, the peak intensity diminished compared with pure Ms. The reason maybe that some channels were blocked, and crystallinity was also weakened, but the mesoporous structure had not been damaged.

The XRD spectra of Ms-La before and after adsorption are shown in Fig. 8. Comparing the two curves, we can see that the diffraction peak obviously changed after adsorption, and the characteristic diffraction peak of $La_2(CO_3)_3$ was weakened, but the peak position did not shift. The new diffraction peak coincided with the standard card JCDP41-0595, which

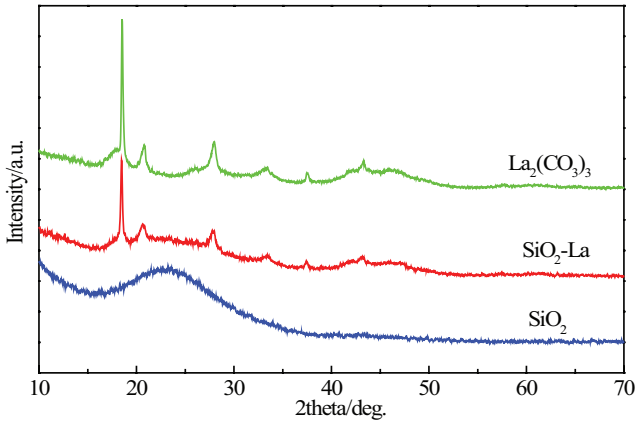

Fig. 7. The XRD spectra of Ms (SiO_2 carrier), pure-$La_2(CO_{3)3}$ and Ms-La (SiO_2-La).

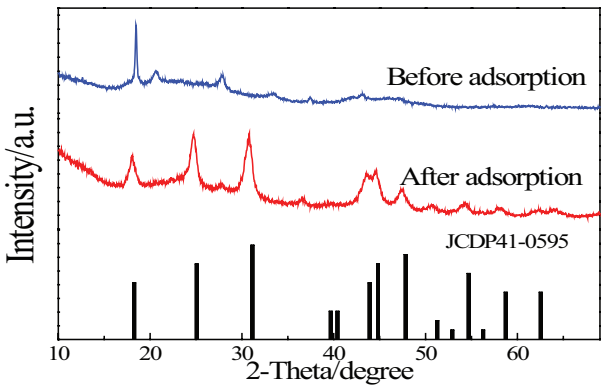

Fig. 8. XRD spectra of the adsorbent before and after adsorption.

showed that $La(CO_3)F$ was formed after the adsorption, at the same time, there was a new diffraction peak which showed that a small amount of LaF_3 was formed.

3.2.3. FTIR analysis

In order to investigate the structure of the materials, the materials were analyzed by FTIR. The FTIR spectra of the SiO_2, Ms-La before the adsorption, pure-$La_2(CO_{3)3}$ and Ms-La after the absorption are shown in Fig. 9. It can be seen that absorption peaks were mainly the characteristic peaks of Ms at 471, 799, 953, 1,075, 1,645 and 3,448 cm^{-1} from Fig. 9(a). According to Fig. 9(b), Ms-La before the adsorption still retained the characteristic peaks of $La_2(CO_{3)3}$ and SiO_2. The strong absorption peak, at 3,438 cm^{-1}, was generated by the crystal water and adsorption water in the sample. Two strong absorption peaks, at 1,300–1,600 cm^{-1}, were stretching vibration of CO_3^{2-} group of carbonate salt. Small absorption peaks, at 600–900 cm^{-1}, were bending vibration of CO_3^{2-} group of carbonate salt. Absorption peak, at 1,075 cm^{-1}, was the frequency of the non-degenerate vibration absorption of carbonate. The most obvious change was the enhancement of the absorption peaks at 799, 953, 1,410 and 1,477 cm^{-1}, and the enhancement and broadening of the absorption peak at 1,075 cm^{-1}. According to Fig. 9(c), the two characteristic peaks of Ms-La before the adsorption at 1,300–1,600 cm^{-1} had changed into a peak after absorption. Due to the fact that fluorine ion substituted carbonate ions during the adsorption process and the strong electronegativity of F^-, the absorption peak at 1,410 cm^{-1} moved to higher frequency and superimposed absorption peak at 1,477 cm^{-1}.

According to the analysis of XRD and FTIR spectra, the main adsorption process is shown as follows:

$$La_2(CO_3)_3 + F^- \rightarrow La(CO_3)F \quad (3)$$

3.2.4. TGDTA analysis

In order to investigate the relationship between quality of the material and the temperature, the materials were analyzed by TG-DTA. The TG-DTA patterns of the Ms-La before the adsorption, Ms-La after the adsorption and Ms are shown in Fig. 10. Compared with Figs. 10(a) and (b), the main process is that $LaCO_3F$ decomposed into LaOF, and the weightlessness rate was 5.99%.

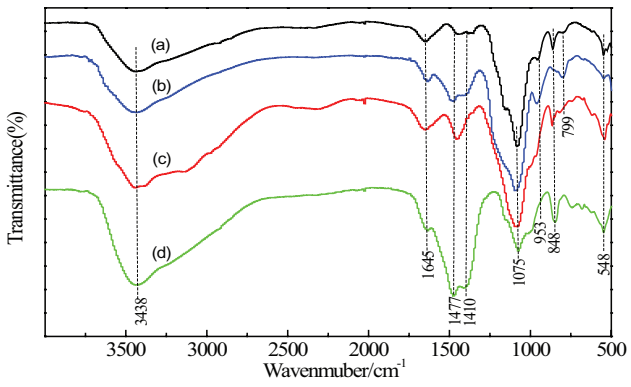

Fig. 9. The FTIR spectra of SiO_2 pure lanthanum carbonate and Ms-La before and after the adsorption.

3.3. The analysis on the adsorption mechanism

3.3.1. Study on the adsorption kinetics

In order to explore the mechanism of the adsorption process, the adsorption kinetics was studied. There were also a lot of dynamic adsorption models, but the most popular dynamic models are quasi-first-order and quasi-second-order kinetic models.

The pseudo-first-order kinetic equation is as follows:

$$\log(Q_e - Q_t) = \log Q_e - k_1 t \quad (4)$$

The pseudo-second-order kinetic equation is as follows:

$$\frac{t}{Q_t} = \frac{t}{Q_e} + \frac{1}{k_2 Q_e^2} \quad (5)$$

When $t = 0$, the initial adsorption rate of h_0 ($mg \cdot g^{-1} \cdot min^{-1}$) can be expressed as follows:

$$h_0 = k_2 Q_e^2 \quad (6)$$

Q_e is the adsorption capacity at adsorption equilibrium (mg/g); Q_t is the adsorption capacity at t (min) of adsorption time (mg/g); t is adsorption time (min); K_1 is the quasi-level adsorption rate constant (min^{-1}); K_2 is quasi-secondary adsorption rate constant [g/(mg/min)].

In the experiment, the experimental data at different temperatures and initial concentrations were fitted by two kinetic models [Eqs. (4) and (5)], and the results are shown in Table 1.

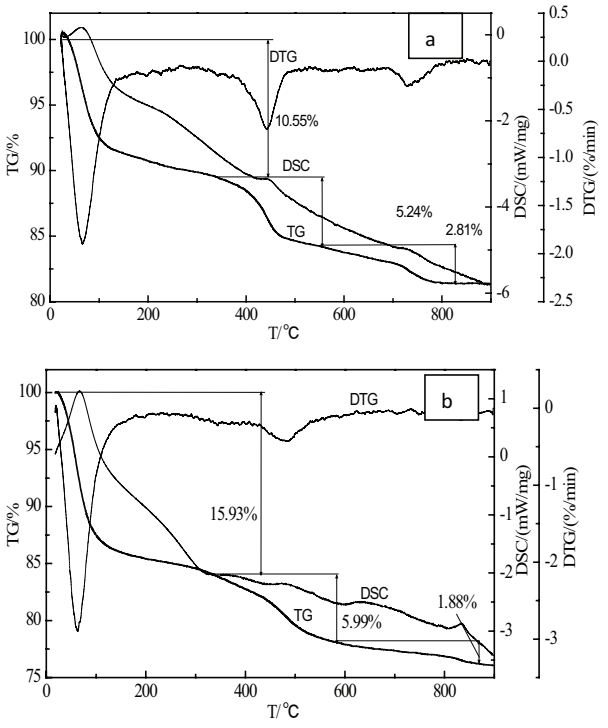

Fig. 10. TG-DTA analysis of Ms-La before the adsorption (a) and Ms-La after the adsorption (b).

From Table 1, it can be seen that the linear fitting correlation coefficient of quasi-second-order kinetic model was greater than 0.9947, and was larger than that of quasi-first order. The measured value of Q_e was closer to fitting values of Q_e. This indicated that the quasi-second-order kinetic model can better describe the adsorption behavior of Ms-La on F^- in water. The kinetic fitting results at different temperatures showed that the correlation coefficient of the adsorption process at different temperatures was greater than 0.9950, and the quasi-second-order kinetic adsorption model can also better describe the adsorption behavior. The adsorption process was controlled by the liquid film diffusion, surface adsorption, particle diffusion, etc. This adsorption model also showed that the adsorption process of F^- was mainly irreversible chemical adsorption.

3.3.2. Study on the adsorption isotherm

Langmuir and Freundlich models are the two common isothermal adsorption models, among a lot of adsorption isotherm models, that can be used to describe the adsorption thermodynamics of liquid–solid system. The Langmuir adsorption isotherm is as follows:

$$\frac{C_e}{Q_e} = \frac{1}{K_L Q_m} + \frac{C_e}{Q_m} \tag{7}$$

Q_m is the saturated adsorption capacity (mg/g); Q_e is the capacity at adsorption equilibrium (mg/g); K_L is related to temperature and adsorption heat of adsorption coefficients, C_e is the adsorption mass concentration at adsorption equilibrium (mg/L).

The Freundlich adsorption isotherm is as follows:

$$Q_e = K_f C_e^{1/n} \tag{8}$$

Q_e is the capacity at adsorption equilibrium (mg/g); C_e is the adsorption mass concentration at adsorption equilibrium (mg/L); n is related to the temperature constant; K_f is Freundlich adsorption coefficient.

The experimental data at different temperatures were fitted by two common isothermal adsorption models, and the results are shown in Table 2. According to Table 2, the correlation coefficient R was greater than 0.9962, so the adsorption isotherm of Ms-La on F^- was more consistent with Langmuir isotherm than that of the Freundlich model. The maximum adsorption capacity was 19.85 mg/g.

4. Conclusion

In this paper, the Ms-La for the fluoride removal performance was characterized by using SEM, XRD, FTIR, and TG-DTA. The adsorption conditions were also investigated. The adsorption performance and capacities of Ms-La were investigated through adsorption kinetics and adsorption isotherm tests. It was found that the removal rate was up to 94.29% at the initial concentration of 10 mg/L, the adsorbent

Table 1
The correlation coefficients of quasi-first order kinetics equation and quasi-second order kinetics equation

Variable		Measured Q_e (mg/g)	Quasi-first-order kinetic equation			Quasi-second-order dynamic equation		
			Q_e (mg/g)	K_1/min^{-1}	R	Q_e (mg/g)	K_2/(g·mg^{-1}·min^{-1})	R
C_{F^-}/(mg/L)	10	7.329	3.360	0.0144	0.9165	8.703	0.0025	0.9950
	20	12.273	4.271	0.0131	0.8685	14.764	0.0012	0.9955
	30	14.882	4.254	0.0113	0.8519	17.538	0.0011	0.9947
T/K	298	7.329	3.360	0.0144	0.9165	8.703	0.0025	0.9950
	308	7.514	2.879	0.0144	0.9365	8.453	0.0040	0.9958
	318	7.421	1.778	0.0113	0.9343	7.838	0.0098	0.9984

Note: R was the linear fitting correlation coefficient.

Table 2
Isothermal adsorption model and its related fitting parameters

T/K	Langmuir isothermal model				Freundlich isothermal model			
	Equation	Q_m (mg/g)	K_l (L/mg)	R	Equation	1/n	K_f	R
298	$Q_e = \frac{5.0406C_e}{1+0.254C_e}$	19.845	0.254	0.9968	$Q_e = 4.235C_e^{0.4162}$	0.4162	4.235	0.9158
308	$Q_e = \frac{9.0573C_e}{1+0.488C_e}$	18.560	0.488	0.9976	$Q_e = 5.126C_e^{0.3629}$	0.3629	5.126	0.8983
318	$Q_e = \frac{13.9797C_e}{1+0.842C_e}$	16.603	0.842	0.9962	$Q_e = 5.190C_e^{0.3371}$	0.3371	5.190	0.8909

Note: R was the linear fitting correlation coefficient.

dosage of 1.2 g/L and the solution pH value of 3. The optimum adsorption time was 180 min and the maximum adsorption capacity could reach 19.85 mg/g. The results of kinetic studies, the analysis of XRD and FTIR spectra showed that the adsorption process was irreversible chemical adsorption. The adsorption of Ms-La for F^- was consistent with the quasi-second-order kinetic adsorption model and the Langmuir isotherm model, which can be used to remove F^- in water at room temperature. The Ms-La prepared by coprecipitation modification had good adsorption effect on F^- removal. Therefore, this composite material can be used to solve the problem of water pollution, and has a wide application prospect in catalytic adsorption, separation and purification, environmental protection.

Acknowledgments

This work was financially supported by National Natural Scientific Fund (No. 21665027), YMU-DEAKIN International Associated Laboratory on Functional Materials, Key Laboratory of Resource Clean Conversion in Ethnic Region, Education Department of Yunnan Province (117-02001001002107).

References

[1] H.B. Wang, M. Yang, J. Wang, Phosphorus adsorption properties of adsorbent of load the lanthanum humic acid, Rare Metal., 5 (2002) 356–359.
[2] L. Chmielarz, P. Kuśtrowski, M. Kruszec, R. Dziembaj, P. Cool, E.F. Vansant, Nitrous oxide reduction with ammonia and methane over mesoporous silica materials modified with transition metal oxides, J. Porous Mater., 12 (2005) 123–129.
[3] L. Fang, F.P. Zhang, Y.X. Jing, J.T. Han, Research on the phosphate removal by consolidated and oxidized lanthanum, Ind. Water Treat., 6 (2010) 11–14.
[4] Z.J. Ma, B.C. Li, Experimental study on the modification of natural zeolite with fluoride removal by, Silicate Bull., 33 (2014) 7–8.
[5] W.F. Han, M. Yang, S.Y. Li, G.Q. Fang, H.B. Wang, On the adsorption of Lonicera on bentonite, J. Yunnan Nation. Univ. (Natural Sci. Ed.), 4 (2008) 343–346.
[6] D. Xue, X.C. Yu, H.X. Sun, Preparation and characterization of MCM-41 mesoporous silica functionalized with sulfonic acid groups, Adv. Mater. Res., 781 (2013) 2606–2611.
[7] J. Min, J.K. Park, E.W. Shin, Lanthanum functionalized highly ordered mesoporous media: implications of arsenate removal, Micropor. Mesopor. Mater., 75 (2004) 159–168.
[8] J. Fan, D. Li, W. Teng, Ordered mesoporous silica/polyvinylidene fluoride composite membranes for effective removal of water contaminants, J. Mater. Chem. A, 4 (2016) 503–506.
[9] Y. Ku, H.M. Chiou, W. Wang, The removal of fluoride ion from aqueous solution by a cation synthetic resin, Separ. Sci. Technol., 37 (2002) 89–103.
[10] M.S. Onyango, Y. Kojima, O. Aoyi, Adsorption equilibrium modeling and solution. Chemistry dependence of fluoride removal from water by trivalent-cation-exchange zeolite, Colloid interface Sci., 279 (2004) 341–350.
[11] M. Ahmadi, R. Yavari, A.Y. Faal, H. Aghayan, Preparation and characterization of titanium tungstophosphate immobilized on mesoporous silica SBA-15 as a new inorganic composite ion exchanger for the removal of lanthanum from aqueous solution, J. Radioanal. Nucl. Chem., 310 (2016) 1–14.
[12] T. Wei, G.Z. Li, T.L. Wang, M. Yang, J.H. Peng, C.J. Barrow, W.R. Yang, H.B. Wang, Preparation and adsorption of phosphorus by new heteropolyacid salt-lanthanum oxide composites, Desal. Wat. Treat., 57 (2016) 7874–7880.
[13] Z.J. Li, B. Hou, Y. Xu, Preparation and characterization of silica-modified titanium dioxide nanoparticles by co-precipitation method, Acta. Phys. Chim. Sin. 2 (2005) 229–233.
[14] L.J. Zhang, X. Hu, C.Z. Yu, R. Crawford, Y. Aimin, Preparation of sinapinaldehyde modified mesoporous silica materials and their application in selective extraction of trace Pb(II), J. Environ. Chem. A., 18 (2013) 9312–9317.
[15] M. Karthikeyan, K.P. Elango, Removal of fluoride from water using aluminium containing compounds, J. Environ. Sci., 11 (2009) 1513–1518.
[16] Y. Qu, C.J. Zhang, P. Chen, Effect of initial solution pH on photo-induced reductive decomposition of perfluorooctanoic acid, Chemosphere, 107 (2014) 218–223.
[17] F. Ge, L. Zhu, Effects of coexisting anions on removal of bromide in drinking water by coagulation, J. Hazard. Mater., 151 (2008) 676–681.
[18] Z. Wang, D.M. Fang, Q. Li, L.Z. Xia, Y. Zhu, H.Y. Qu, Y.P. Du, Modified mesoporous silica materials for on-line separation and preconcentration of hexavalent chromium using a microcolumn coupled with flame atomic absorption Spectrometry, Anal. Chim. Acta., 24 (2012) 725–735.